

Histological and Ultrastructural Changes of the Brain, Pancreas and Ileum of diabetic and nondiabetic mice under heat stress with special reference to heat shock proteins.

Hamdy Hamed Swelim

Department of Zoology , Faculty of Science Ain Shams University

Abstract

The current study was designed to evaluate the thermal stress effect on brain, pancreas and ileum in normal and alloxan-diabetic mice by studying the structural changes at both light and electron microscopical levels and by studying the molecular changes expressed through the examination of protein banding pattern in the electrophorograms of the different groups . The animals were divided into four main groups; control mice, alloxan diabetic mice, heat-stressed nondiabetic mice and heat-stressed diabetic mice.

No remarkable changes could be detected in nonstressed diabetic animals except the ultrastructural changes noticed in B cells of islets of Langerhans in pancreas. The heat-stressed nondiabetic animals displayed various cellular and subcellular changes in the organs of study, which were focal in most of the cases. Signs of restitution were also noted in the three selected organs in this group . On the other hand, heat stress was so much destructive in diabetic mice and that was so clear specially in pancreas. The difference in degree of cellular injury between diabetics and nondiabetics is correlated with data of protein studies which demonstrated more expression of heat stress proteins (HSPs) in nondiabetics and attenuation of this expression in diabetics. These stress proteins are suggested to play an important role in protection against thermal stress injury. Consistent with this, the brain which showed more expression of HSPs was the least affected of the three organs. Moreover, the attenuated expression of these HSPs in diabetics highlights the suggestion that diabetes deranged the stress response and delayed the expression of the protective HSPs.

In conclusion further studies are needed to characterize the molecular structure of the HSPs and the genes responsible for the expression of these proteins in these tissues and the other body tissues .

Introduction

The exposure of human being to heat stress is widespread specially among the military people during military maneuvers, in various industries, specially those using high temperature furnaces like metallic industries, in ordinary bakeries (specially those in rural areas), also in hot storms during the summer and sometimes during radiotherapy.

Mammalian cells die after hyperthermia in a time-temperature-dependent manner and cell death occurs within hours. Therefore, a considerable current interest in combining hyperthermia with various ionizing radiation protocols in order to increase the effectiveness of radiotherapy is greatly increasing (Haschek and

Rousseaux, 1991). On the other hand, nonlethal heat stress causes subcellular changes in macromolecules, destabilization of multimolecular structures, and induction of increased rates of metabolic reactions followed by disregulation of these reactions (Kelty *et al.*, 2002). All these reactions are named stress response, which is a universal mechanism developed by all organisms to deal with adverse changes in environment, which lead to synthesis of stress proteins. Moreover, exposure of cells to nonlethal heat shock results in transient resistance to subsequent exposures at elevated temperatures (Gabriel *et al.*, 2002). The complications which usually develop in humans and in animals after thermal injury are

varied and poorly understood besides the role and mechanism of the action of stress proteins are still debatable .

The purpose of the present study was to characterize the structural and ultrastructural changes that would be caused by heat stress in three different tissues ; brain, pancreas and ileum and the possible induction of heat shock proteins through the activation of heat shock genes. The rationale for this study lies in the yet unresolved controversy of the role of these inducible proteins in cell survival from various stresses. A further aim was to investigate the degree of damage caused by heat stress on diabetic animals and the extent of heat shock protein expression and its relevant heat stroke tolerance in diabetics.

Materials and Methods

About 40 male CD-1 mice weighing 25 to 30 g were used in this experiment. The animals were kept under standard environmental conditions (except the heat-stressed) and were given rodent chow and water ad libitum . They were divided into four main groups; control, alloxan-induced diabetics, nondiabetic – heat stressed and diabetic-heat stressed. Food was withheld from the mice of the second group 3-4 hours prior to alloxan administration. Then for the induction of diabetes, alloxan was injected subcutaneous at 75 mg/kg body weight in the saline (According to Heikkila. and Cabbat, 1980). Animals from this group were tested for diabetes and decapitated 3 days post alloxan injection. Mice of the third group (nondiabetic heat-stressed) were subjected to thermal stress at 38°C +0.5 and 75-80% humidity for 2 hrs daily for the period of one week and the diabetic mice of the fourth group were subjected to thermal stress in the same regimen . For light microscopical preparations, animals were decapitated and brain, pancreas and ileum were quickly fixed in 4% phosphate buffered paraformaldehyde, then washed and processed for paraffin procedures . Serial paraffin sections of 7 um in thickness of

brain were stained with cresyl violet and haematoxylin and eosin stains . Glial cells were demonstrated by using the silver method of Scharanberg (1954) and Weil and Davenport (1933) for astrocytes and microglia respectively. Glycol methacrylate embedding was applied to get semithin sections of pancreas and ileum that were stained with toluidine blue, paraldehyde fuchsin (for pancreatic islets), basic fuchsin-methylene blue stain (Bennett *et al.*, 1976) and alcian blue –PAS . For ultrastructural study tissues were dissected out into very small pieces , fixed in 3%glutaraldehyde , postfixed in 2% Osmium tetroxide , dehydrated and embedded in Epon 812 . Semithin sections were stained with toluidine blue while ultrathin sections were cut at 60 nm by using a diamond knife and stained with uranyl acetate and lead citrate then examined by Jeol EX 1200 transmission electron microscope .

For protein studies SDS polyacrylamide gel electrophoresis was achieved using the standard method of Laemmli (1970). Brain, pancreas and ileum tissues were quickly removed and homogenized in (1:3 w/v) cold 0.32 M sucrose solution which contained protease inhibitors. Homogenates were centrifuged at 20,000 RPM for one hour, then one volume of each supernatant was mixed with 2 volumes of Laemmli's sample buffer and heated at 100 degree for 5 minutes. Molecular weight markers (Technical Bulletin No.877 Sigma) of the range 14,400 to 94,000 daltons were used. Slab gels were stained with coomassie brilliant blue according to Neuhoff *et al.*(1988). Molecular weight of the extraprotein bands was estimated from the calibration curve made for each gel.

Results

Histological and Ultrastructural Studies :

The brain, pancreas and ileum are the organs selected for the present study at both the light and electron microscopy levels.

Brain in control :

In control mice the brain shows normal basic histological structures in all

Histological and Ultrastructural Changes of the Brain.....

the levels, and that appears through the examination of serial paraffin sections stained with cresyl violet and Hx & E and semithin sections stained with basic fuchsin-methylene blue stain. The cerebral cortex shows normal appearance of the vascular endothelium and the different types of neurons and glial cells which appear in obviously arranged distinct layers (Fig. 1). Ultrastructural investigations reveal normal subcellular structure of the pyramidal and nonpyramidal neurons, with their relatively large euchromatic nuclei which usually possess up to three nucleoli. The nucleolus displays the electron dense fibrillar form with electron lucent areas inbetween and sometimes found associated with "satellites", which represent the heterochromatic X chromosome of the females (Fig. 2). Several profiles of Golgi apparatus take the perinuclear position, and the cytoplasm appears highly rich in mitochondria, rough endoplasmic reticulum and numerous polysomes (Fig. 2). The major three types of glial cells; astrocytes, microglia and oligodendrocytes are clearly demonstrated in cresyl violet stained paraffin sections and specific silver impregnation methods (Figs 1 and 3). Astrocytes appear star shaped with their branching processes that sometimes send "endfeet" processes to blood vessels, while microglia appear cylindrical in shape with few slender processes (Figs. 3a,b).

Brain in treated groups :

Examination of serial brain sections taken from alloxan-diabetic mice did not show any obvious pathological lesions or damage neither at the light microscopical or electron microscopical levels.

In heat-stressed nondiabetic mice focal inflammatory areas, filled with polymorphs and lymphocytes, were noticed in the neocortex, mostly lying peripheral beneath the pial surface (Fig. 4). A second remarkable feature noted was the appearance of edema in various regions of the brain including neocortex and hippocampus (Fig. 5). Light microscopical examination of the brain sections showed obvious increase in the amount of oligodendrocytes specially in cerebral

cortex (Fig. 5). Sometimes blood vessels were found detached from the surrounding tissue leaving perivascular vacuoles (Fig. 6a). Frequently, lesioned neurons specially the small pyramidals were found shrunked, darkly stained and lost their neural processes (Fig. 6b). By electron microscopy, it was found that the damaged cells possessed greatly degenerated mitochondria which appeared as electron lucent swollen vacuoles, which might be due to edema, containing only the debris of fragmented cristae (Fig. 7). Golgi sacs were prominently dilated, disorganized and their limiting membranes appeared ruptured leaving the interiors of the sacs fused together. The nucleus became highly irregular, slightly more heterochromatic than in control, contained very electron dense intact nucleolus, while the remaining cytoplasm was still filled with highly electron dense ergastoplasm (rough endoplasmic reticulum and ribosomes) (Fig.7).

In heat-stressed diabetic mice the most striking feature was the extensive edema and shrinkage of almost all the neurons in neocortex, that made each neuron being surrounded by a clear halo with loss of almost all of their extending processes (Fig.8) and the loss of grey-white matter discrimination in various regions of the brain. Also the blood vessels were found surrounded by clear wide spaces. Ultrastructural investigations revealed that there were variable degrees of damage among the various types of neurons in the different brain regions. The most severe damage was that noticed in neurons of the neocortex and hippocampus as they displayed severe chromatolysis, loss of most of the rough endoplasmic reticulum while the rest of the organelles were no more seen. Nuclei were karyolysed and lost their characteristic spherical profile with the double leaflet nuclear envelope (Fig.9). Neurons from the hypothalamus were not severely damaged like those of the cortex, as they were still possessing the intact nucleus but with irregular contour and more electron dense chromatin. All the mitochondria were swollen electron lucent and lost all of their cristae, Golgi cisternae were swollen and damaged while the rest of cytoplasm contained electron dense ribosomal

substance consisting of compact rough endoplasmic reticulum and polyribosomes (Fig. 10).

Pancreas in control :

The pancreas as a mixed endocrine and exocrine gland appears in semithin and paraffin sections formed of main functional units called acini, representing the exocrine part and scattered round or ovoid clusters of cells which are the islets of Langerhans representing the endocrine part (Fig.11a,b).

At the light microscopical level, semithin sections stained with toluidine blue reveal that each acinus is composed of pyramidal shaped cells, the acinar cells, whose apical cytoplasm appears packed with numerous dark blue spherical zymogen granules (Fig. 11a). The striking feature of these acinar cells is that the distribution of the cytoplasmic organelles is highly polarized, where the basal cytoplasm contains the nucleus and is highly basophilic due to the distribution of the rough endoplasmic reticulum which appears as abundant parallel cisternae studded with many attached ribosomes (Fig.12). Inbetween the adjacent cisternae of rough endoplasmic reticulum, there are free ribosomes and numerous mitochondria. The well developed Golgi apparatus lies in the supranuclear area and above which are found numerous zymogen granules that extend to occupy most of the apical cytoplasm. These zymogen granules are bounded by smooth layer and have a homogeneous electron-dense content. They occupy more than 50 % of the volume of the cell (Fig.11a) .

The islets of Langerhans (mostly about 100-200 μm in diameter)are demarcated from the surrounding pancreatic acini by a delicate investment of reticular fibres . They appear randomly distributed between pancreatic acini but they tend to be more concentrated in the tail region (splanchnic portion) of the pancreas . In stained semithin and paraffin sections they appear paler than acinar cells and arranged in irregular cords between which is found abundant capillary bed (Fig.11b). The major cell types of the islets are A (alpha) and B (beta) cells which can be

differentiated by the special staining method of paraldehyde fuchsin after strong oxidation with acidified pot. permanganate . In glycol methacrylate semithin sections stained with basic fuchsin-methylene blue the B cells take the blue colour and they are the most numerous of the islet cells while the A cells appear faintly stained (Fig.11b). A third type called protein producing cells (pp) or F cells is also found but in very few numbers (Fig.13a). Ultrastructurally, the B cell is characterized by the numerous secretory vesicles (about 300 nm in diameter) containing electron dense core surrounded by clear halo. The nucleus is heterochromatin rich with irregular contour, while the rough endoplasmic reticulum and ribosomes are not readily distinguishable due to the engorgement of the cells with the secretory vesicles . However, spherical mitochondria and small Golgi apparatus can be clearly distinguished (Fig.13a). The A cell is differentiated from B cell by its smaller secretory vesicles(about 200 nm in diameter) which usually lack the clear halo that surround the dense core and is characterized also by the obviously indented and sometimes lobulated nucleus (Fig. 13b) . The F cells (pp cells) can be distinguished ultrastructurally by their characteristic small electron dense secretory vesicles (about 100-200 nm in diameter) and their processes which extend between the B cells (Fig. 13a) .

Pancreas in treated groups :

In alloxan-diabetic mice, no structural or ultrastructural alterations could be detected in acinar cells if compared with control, moreover they were found containing the characteristic abundant zymogen granules. However, the islets of Langerhans displayed some degenerative changes included diminution of the size of islets, marked reduction in the number of B cells with obvious ultrastructural changes (Fig.14). They showed extensive degranulation and great damage of the nucleus which lost the nuclear membrane and great amount of the heterochromatin , while the rest of euchromatin became patchy in appearance with several vacuolated areas . Apoptotic bodies were also frequently

Histological and Ultrastructural Changes of the Brain.....

observed in the cytoplasm which became devoid of any intact organelles. Adjacent A cells appeared intact containing the mitochondria, Golgi apparatus, few cisternae of rough endoplasmic reticulum and the characteristic secretory vesicles which appeared with narrow halo surrounding a dense core (Fig. 14).

The remarkable features noticed in acinar cells of the nondiabetic heat-stressed mice were the depletion of zymogen granules and presence of numerous vacuoles similar in size to that of the zymogen granules or slightly bigger. Some of these vacuoles appeared containing small centrally located zymogen granule in each (Fig.15). Electron microscopical investigations revealed that some of these vacuolated cells contained large number of damaged electron lucent spherical or ovoid mitochondria of nearly the same size like zymogen granules (Fig.16). This might suggest that vacuolar degeneration in these cells is likely to be due to the mitochondrial degeneration in addition to depletion of zymogen material. Also of interest is that in such cells, the rough endoplasmic reticulum was dilated and lost the characteristic parallel array pattern and transformed into concentric whorls – like arrays with the appearance of myelin figures (Fig.16). Nuclear changes were in the form of severe to moderate dilation of the perinuclear space, and frequent appearance of pyknotic nuclei. Light microscopic and ultrastructural examination revealed the presence of numerous interacinar and periductal interstitial cells filled with membrane bounded vacuoles, numerous small vesicles, coated vesicles, polyribosomes and few mitochondria (Fig.17). Basal plasma membrane of acinar cells showed peculiar numerous microvilli-like processes. No remarkable changes could be distinguished in cells of islets neither at the light nor the electron microscopical levels.

In heat-stressed alloxan-diabetic mice semithin sections of, Epon and glycol methacrylate embedded samples together with ultrathin sections revealed several manifestations of cellular lesions in pancreatic acini. The severity of cellular injury varied between acini and even within the

acinus. The most prominent feature was the appearance of focal necrotic areas where pyknotic nuclei were more frequently observed specially in tail region of the pancreas. By light microscopy, damaged cells were found greatly shrunk, possessed numerous vacuoles and pyknotic nuclei and in the meantime adjacent acini appeared intact with mild vacuolation (Fig.18a). Ultrastructural investigation of these damaged cells, made clear cut that vacuolization is due to the swelling and degeneration of most of the mitochondria, which sometimes appeared containing myelin figures. Nuclei displayed chromatin clumping and margination in some cells while others were entirely pyknotic. A peculiar form of interdigitation taking the form of ball and socket was noted between adjacent lesioned acinar cells (Fig.18b). Although these cells retained the normal parallel array pattern of rough endoplasmic reticulum, zymogen granules were found greatly depleted. A second form of lesion was noted by electron microscopy, where some acinar cells were found containing markedly dilated, vesiculated rough endoplasmic reticulum forming megacisternae and decreased number of membranous arrays besides having intracisternal sequestration. Some of the mitochondria lost their cristae and contained finely fragmented debris instead (Fig.19a). A third form of lesions appeared in the form of massive accumulation of apoptotic bodies of variable sizes. Such apoptotic bodies were in the form of vacuoles containing nonhomogeneous zymogen-like materials, intact zymogen granules and sometimes sequestered portions of rough endoplasmic reticulum (Fig.19b). Strikingly, rough endoplasmic reticulum in the remaining cytoplasm appeared in its normal fingerprint-like form.

Centroacinar cells as seen by electron microscopy displayed a great dilatation of the space lying between the two leaflets of the nuclear envelope creating large vesicles that fused with degenerated mitochondria. Numerous collagen fibres were also noted surrounding the cells. Nucleus became highly irregular in shape and its chromatin became condensed and marginal in position (Fig.20).

Blood capillaries also displayed a peculiar electron dense reticulum-like endothelium filled with numerous microvesicles (Fig.21). Ductal epithelium was highly disorganized and the cells possessed extensive apical microvilli and basal processes, while their nuclei became abnormally lobulated. Intercellular spaces between ductal cells increased greatly and sloughed cellular masses of ductal epithelium were noted. Marked increase in interstitial cell populations was detected with coexistence of fibroblasts and numerous collagen fibres in the interacinar regions (Fig. 22). Heat stress provoked degranulation of most of the islet cells. The cells showed two forms of lesions ; the first form appeared fragmented, with deformed nuclei and lost most of the secretory vesicles and numerous collagen fibres were accumulated (Fig.23). The second form appeared with numerous empty secretory vesicles, large masses of myelin figures and nucleus was surrounded by a very wide clear halo while Golgi sacs were still intact (Fig.24) .

Ileum in Control :

The lining of the ileum appears by light microscope studded with innumerable villi that give it a velvety appearance . They are essentially fingerlike or leaflike evaginations of the mucosa, so they greatly increase the absorptive surface (Fig. 25). At their bases simple tubular invaginations or pits can be distinguished which extend to the muscularis mucosa but don't penetrate it; these pits are the intestinal glands, or crypts of Lieberkuhn. The epithelium of the villi is continuous with that of the crypts forming a continuous sheet. The core of villi is highly rich in connective tissue (lamina propria) and cells of immune system. The simple columnar epithelium that lines the crypts and covers villi is distinguished into four main types of cells; the absorptive cells, goblet cells, enteroendocrine cells and at the bottom of the crypts lie the Paneth cells, which have the cytological characteristics of protein-secreting zymogenic cells (Figs.25-29) .

The absorptive cells are tall and columnar with oval nuclei, which are mostly euchromatic with peripheral

heterochromatin, located in the lower half of the cells and the cells display apical striated or brush border which consists of minute rodlike microvilli in a parallel array (about 3600 microvillus per each cell) (Fig.26). The brush border is PAS-positive because of a thick surface coat on the microvilli that is rich in glycoproteins (glycocalyx) (Fig.25). The polarity of the absorptive cells is evident in structural differences between the free and attached surfaces and also in the distribution of the organelles. As it can be noticed that luminal surface is composed of closely packed microvilli; the subjacent cytoplasm is organelle free forming the terminal web, below which are found elongated mitochondria, rough and smooth endoplasmic reticulum. In the supra nuclear area lies the Golgi apparatus. The lateral cell surfaces are closely apposed and sometimes appear folded or forming interdigitation processes (Fig.26) .

The second type of epithelial cells is the goblet cells which are recognized by their basophilic cytoplasm, basally located nuclei, and the accumulation of mucous secretory granules that fill and distend their apices. Their content is alcian blue, PAS and metachromatic-positive indicating the acidic glycoprotein nature (Figs.25) .

Enteroendocrine cells are frequently noticed through the electron microscopical examination and are characterized by the small (about 200-250 nm in diameter) electron dense rounded or oval granules which are nearly similar to those in islets of Langerhans or pituitary cells. Their nuclei are slightly irregular with peripheral heterochromatin and the cytoplasm appears electron lucent containing few cisternae of endoplasmic reticulum and elongated mitochondria (Fig.27).

The protein producing Paneth cells are usually found at the base of the intestinal crypts and appear in semithin sections filled with large dark blue granules after staining with toluidine blue (Fig. 28). By electron microscopy they appear pyramidal in shape having the same cytological features of the acinar cells of pancreas, with large acidophilic electron dense granules (about 1000-2000 nm in diameter) in the apical cytoplasm while the basal cytoplasm

Histological and Ultrastructural Changes of the Brain.....

contains the well developed cisternae of rough endoplasmic reticulum taking a typical fingerprint-like appearance (Fig. 29). Nuclei are variable in shape due to the continuous secretory function but they are all heterochromatin-rich. The supranuclear area appears in electron micrographs occupied by many active Golgi apparatus profiles enclosing different stages of immature secretory vesicles. Mitochondria are found distributed mostly in the mid-region between the apex and nucleus (Fig.29).

Ileum in treated groups:

The epithelial lining of the ileum in alloxan-diabetic mice was so much similar to that in control animals at both the light and electron microscopical levels and no remarkable changes were noted. In heat-stressed nondiabetic mice, remarkable increase in the number of goblet cells was noticed (Fig.30), in addition an obvious increase in the number of mitotic figures was also noted in the intestinal crypts, with hypercellularity and increase of lymphocytes in submucosa (Fig.31). The previous features were noted in the ileum regions close to the duodenum, while in the distant ileum other forms of changes were noted. The striking feature was the vacuolization of the basal cytoplasm in virtually all ileal absorptive cells, mostly in the upper half of the villi. The general villus shape was somewhat scalloped and showed blebbing (Fig.32). By electron microscopy, the remarkable features noted in absorptive epithelium were the basal vacuolization, irregularity of the nuclei which became no more basal in position and the decrease in the number density of microvilli (decreased to about 1600 per each cell compared with 3600 in control) which lost their parallel array form (Fig.33). However the cells retained the rest of the organelles in intact form. On the other hand, crypt cells showed no ultrastructural changes.

The most remarkable feature observed in heat-stressed alloxan-diabetic mice was the extensive sloughing off in cells from the villi tips in addition to blebbing (Fig.34). By electron microscopy the absorptive cells displayed the same blebbing and extensive loss of the microvilli with rupture of plasma

membrane and sequestration of damaged mitochondria by circular elements of rough endoplasmic reticulum, thus losing the parallel array pattern and creating dilated intracisternal wide spaces (Fig.35). Paneth cells were greatly damaged, some of them were completely lysed and others lost their organelles and remained with little vacuolated cytoplasmic rim with highly shrunk irregular nuclei (Fig.36).

Protein study :

Protein content of the brain, pancreas and ileum was studied using the method of SDS polyacrylamide gel electrophoresis which showed that the protein extracts from these organs were characterized by specific banding pattern for each organ (Fig.37). Electrophorograms of the heat-stressed nondiabetic mice were characterized by the appearance of extraprotein bands that lie in the range of 60-110 kilodaltons. The extrabands in brain electrophorograms were nearly of about 110 kilodaltons and appeared as double bands, while in case of pancreas and ileum the extrabands lied nearly in the range of 67 kilodaltons. On the other hand, the banding pattern of the diabetic heat-stressed animals was nearly similar to that of the control (Fig.37) and the extraprotein bands are not clearly demonstrated which reflects the attenuating effect of diabetes on protein synthesis of these stress related proteins.

Explanation of Figures

Figures 1-3 are for control brain tissue structures :

Fig.1 : Paraffin cross section of cerebral cortex showing the arrangement of the pyramidal neurons in distinctive layers (arrows) inbetween which are found layers of nerve fibres (arrow heads). Small oligodendrocytes can be distinguished (small arrows). Cresyl Violet. (original magnification 200 x)

Fig.2 : Electron micrograph of a pyramidal neuron showing the large euchromatic nucleus with large nucleolus (nu) associated with two satellites (arrows) and the cytoplasm is filled with rough endoplasmic reticulum (er), polysomes (arrow heads)

and mitochondria (m). Golgi apparatus takes the perinuclear position (g).

(X10000)

Fig.3 : Astrocytes and microglia in cerebral cortex.

(a) The astrocytes are star shaped with end-feet processes on surface of blood vessels (b.v.) Silver method of Scharanberg .

(Original magnification. X 1000)

(b) Microglial cell with small cylindrical body and few slender processes. Silver method of Weil and Davenport .

(Original magnification. X 1000)

Figures from 4-7 are for brain in heat-stressed nondiabetic mice :

Fig.4 : Paraffin cross section of cerebral cortex showing focal inflammatory areas filled with polymorphs and lymphocytes (arrows). Hematoxylin and eosin (Original magnification. X 100).

Fig.5 : Paraffin cross section of cerebral cortex showing obvious edema in neocortex (arrows) and increased number of oligodendrocytes (arrow heads). Cresyl violet (original magnification X 200)

Figs.6a,b: (a) Semithin sections of cerebral cortex showing perivascular vacuoles (arrows). (original magnification X 400)

(b) Small pyramidal neurons appear shrunk and darkly stained. Basic fuchsin – Methylene blue (original magnification X 1000)

Fig. 7 : Electron micrograph of two pyramidal neurons in the cortex. Mitochondria (m) are swollen and electron lucent, Golgi apparatus (g) is dilated with ruptured membranes and fused intracisternal spaces. Nucleus is highly irregular with very electron dense intact nucleolus (nu), while the cytoplasm is filled with rough endoplasmic reticulum (arrows).(X15000)

Figures from 8-10 are for brain in heat-stressed diabetic mice :

Fig.8 : Paraffin cross section of cerebral cortex , showing extensive edema and shrinkage of almost all of the neurons. Cresyl Violet (Original magnification X 200)

Fig. 9 : Electron micrograph of small pyramidal neurons from the cerebral cortex showing severely damaged one (arrow),

which lost all the organelles and the nuclear envelope while the nucleus is almost karyolysed. (X 13000)

Fig.10 : Electron micrograph of a large multipolar neuron from hypothalamus which possess intact nucleus but with irregular contour. Mitochondria (m) and Golgi apparatus (g) are greatly damaged, while rough endoplasmic reticulum is still intact. (X10000)

Figures from 11-13 are for control mice pancreas :

Fig.11 : Semithin sections of pancreas showing :

(a) The exocrine part formed of numerous acini (arrows), each acinus is composed of pyramidal shaped cells whose apical cytoplasm is packed with numerous zymogen (blue stained) granules (arrow heads) while the nuclei are basal in position.

Toluidine blue (original magnification X 200)

(b) The endocrine part in the form of round cluster of cells surrounded by thin reticular sheath (arrow head) and inbetween which are found small capillaries (arrows). The B cells appear darkly stained while the A cells are lightly stained (small arrow).

Basic fuchsin –methylene blue (original magnification X 200)

Fig. 12 : Electron micrograph showing acinar cell in pancreas. The nucleus is basally located and surrounded by rich parallel rough endoplasmic cisternae inbetween which lie mitochondria (m) and the apical region is studded with zymogen granules (zg). Microvilli (mv) project into the acinar lumen (star). (X 15000)

Fig.13 : Electron micrograph showing part of the islet of Langerhans.

a- B cells characterized by the numerous secretory vesicles containing electron dense core, few mitochondria (m) and Golgi cisternae (g). part of F cells are found characterized by the small electron dense secretory vesicles (arrows). (X 8000)

b- A cells characterized by the numerous secretory vesicles which usually lack the clear halo that surround the dense core and the indented nucleus. (X 8000)

Histological and Ultrastructural Changes of the Brain.....

Fig.14 : Electron micrograph of islet cells from an alloxan-diabetic mouse, showing degranulated B cell (B) with damaged nucleus (n) and containing apoptotic body in cytoplasm (ap). Adjacent A cell shows minor changes in secretory vesicles which appeared with narrow halo while mitochondria (m) and Golgi apparatus (g) are intact. (X 15000)

Figures from 15-17 are for pancreas in heat-stressed nondiabetic mice :

Fig. 15 : Semithin section of pancreas showing depletion of zymogen granules and appearance of numerous vacuoles some of which contain small granules. (Basic fuchsin-methylene blue X 1000)

Fig.16 : Electron micrograph showing part of acinar cell. Rough endoplasmic reticulum is greatly dilated and most of the mitochondria (m) are swollen and degenerated. Few zymogen granules are still found (arrows) and myelin figures can be noticed inbetween cisternae of the er (arrow heads). (X 20000)

Fig. 17 : Electron micrograph showing interacinar interstitial cell in the pancreas. The cytoplasm is lighter than the surrounding 3 acinar cells and is filled with membrane bound vacuoles, small vesicles (arrows), coated vesicles (arrow heads), mitochondria (m) and polyribosomes (rb). Acinar cell basal membrane display microvilli - like processes. (X 15000)

Figures from 18 to 24 are for Pancreas from heat-stressed diabetic mouse :

Fig.18 : (a) Semithin section showing some necrotic acinar cells with pyknotic nuclei (arrows) and vacuolated cytoplasm, while other acini showed mild vacuolation (arrow head). Basic fuchsin-methylene blue (original magnification X 400).

(b) Electron micrograph showing ultrathin section from the same region of the previous figure sample showing three necrotic acinar cells with completely degenerated mitochondria (m), some of them contain myelin figures (arrows) and nuclei show different stages of pyknosis. A peculiar ball and socket interdigitation occur between adjacent acinar cells (arrow

head), while rough endoplasmic reticulum is intact. (X 10000)

Fig. 19 : (a) Electron micrograph showing a second form of damage where the rough endoplasmic reticulum appeared dilated, vesiculated and form megacisternae with decreased number of membranous arrays. (X 4000)

(b) Electron micrograph showing a third form of damage where the cytoplasm appear filled with large and small apoptotic bodies (arrows) containing nonhomogeneous zymogen-like materials, intact zymogen granules and portions of rough endoplasmic reticulum (arrow head). The rest of cytoplasm contained the typical fingerprint like rough endoplasmic reticulum. (X 10000)

Fig.20 : Centroacinar cell with irregular nucleus, highly dilated perinuclear space that lie between the two leaflets of nuclear envelope and scanty degenerated cytoplasm surrounded by collagen fibers (arrows) (X 24000)

Fig. 21 : Electron micrograph showing a blood capillary with damaged endothelium (arrow), ductal epithelium shows sloughed cellular masses (arrow head) and wide intercellular spaces (thick arrows) X 8000

Fig.22 : Fibroblast in the interacinar region with extensive processes (arrows) and dense bed of collagen fibres (arrowheads). (X 10000)

Fig.23 : Electron micrograph showing greatly damaged islet cells, fragmented (arrow) or degranulated (arrow head) with appearance of numerous collagen (small arrows). (X 8000)

Fig.24 : Slightly damaged islet cells showing empty secretory vesicles (arrows), large perinuclear halo and large masses of myelin figures (arrow head), while Golgi sacs are still intact (g). X 12000

Figures 25 to 29 are for ileum from control mice:

Fig.25 : Transverse semithin section showing columnar intestinal epithelium lining the crypts (in the upper half) and covering the villi (in the lower half). Nuclei are oval basally located (arrows), goblet cells take the alcian blue colour, dense lamina propria fill the interior of

the villi and the glycocalyx take the + ve PAS (magenta colour).

Glycol methacrylate – embedding. Alcian blue – PAS – methylene blue stain.

(original magnification X 200)

Fig.26 : Electron micrograph showing the absorptive epithelial cells with their characteristic microvilli, organelle free terminal web (arrow head), elongated mitochondria (m), rough endoplasmic reticulum (arrows), supranuclear Golgi apparatus (g) and lateral interdigitation processes (thick arrows). X 5000

Fig.27 : Electron micrograph showing an enteroendocrine cell characterized by the small electron dense rounded or oval granules, slightly irregular nucleus and cytoplasm with few mitochondria (m) and rough endoplasmic reticulum (arrow). X 6000

Fig.28 : Semithin section showing Paneth cells in crypts of Lieberkuhn they appear pyramidal in shape filled with dark blue granules that accumulate in the lumen of the crypt while the nuclei are basal in position.

Toluidine blue (original magnification X 1000)

Fig.29 : Electron micrograph showing Paneth cells with apical large electron dense granules, basal cytoplasm is filled with fingerprint – like endoplasmic reticulum, supranuclear Golgi apparatus (g) and mitochondria in the mid region (m)

(X 6000)

Figures from 30 to 33 are for ileum from heat-stressed nondiabetic mice.

Fig.30 : Semithin glycol methacrylate section stained with Toluidine blue showing increased goblet cells with pink metachromasia .Toluidine blue (original magnification X 400)

Fig.31 : Semithin Epon section showing increased mitotic figures (arrows) and hypercellularity in the region of intestinal glands. Toluidine blue (original magnification X 200).

Fig. 32 : Semithin section showing extensive basal vacuolization of the intestinal epithelium (arrows), blebbing of the villi tips (arrow head) which took the scallop shape. Toluidine blue (original magnification X 200)

Fig.33 : Electron micrograph showing absorptive epithelial cells with basal vacuolization (arrow heads), displacement of nuclei from basal position and decreased number of apical microvilli (arrows).

(X 4500)

Figures from 34 to 36 are for ileum from heat-stressed diabetic mice :

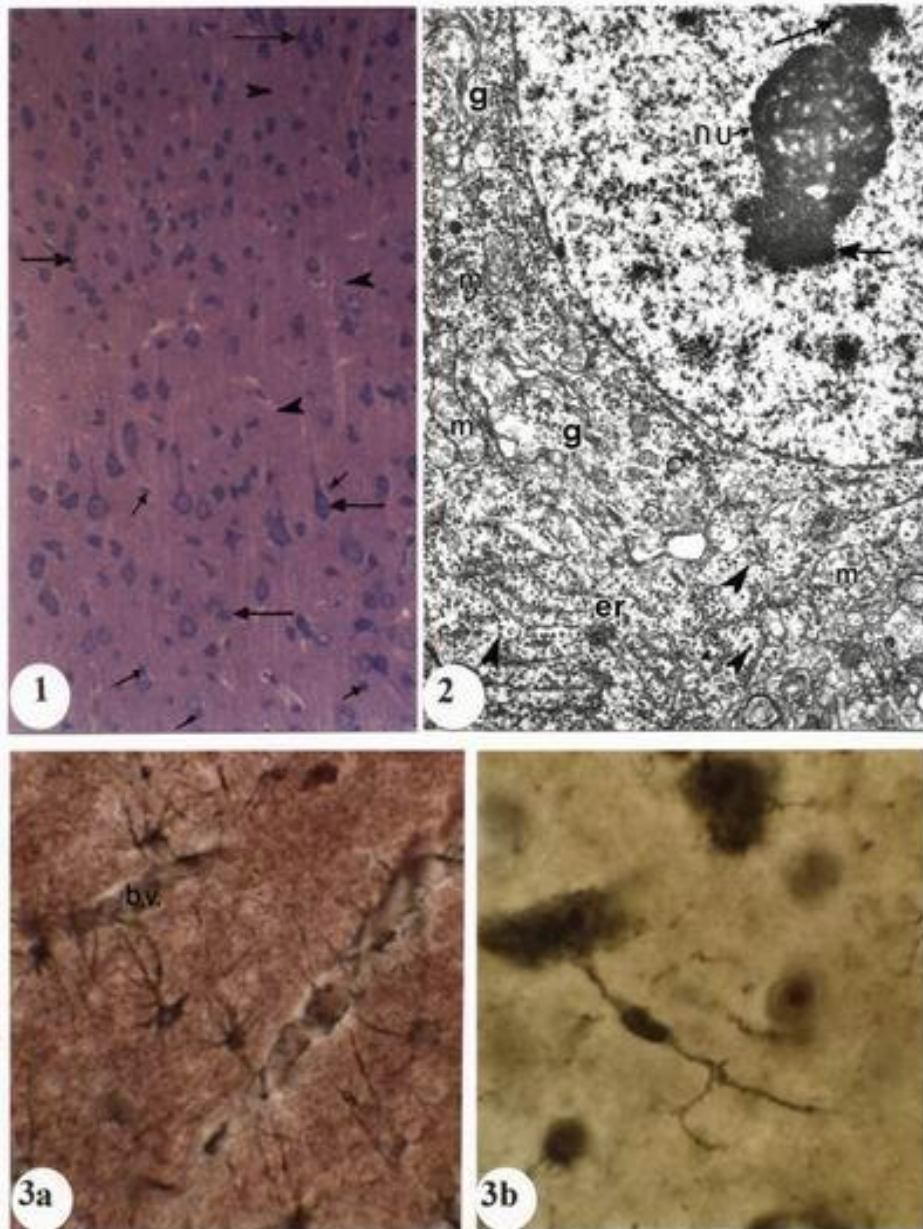
Fig.34 : Semithin section showing extensive sloughing off of villi tips and blebbing (arrows). Toluidine blue (original magnification X 200)

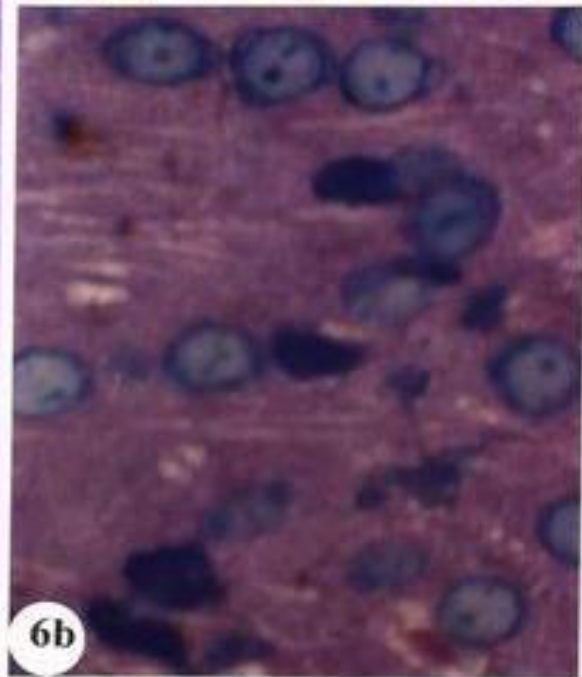
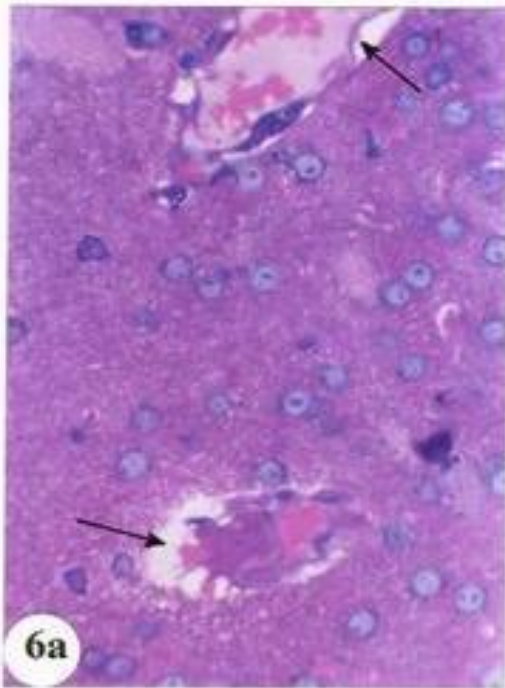
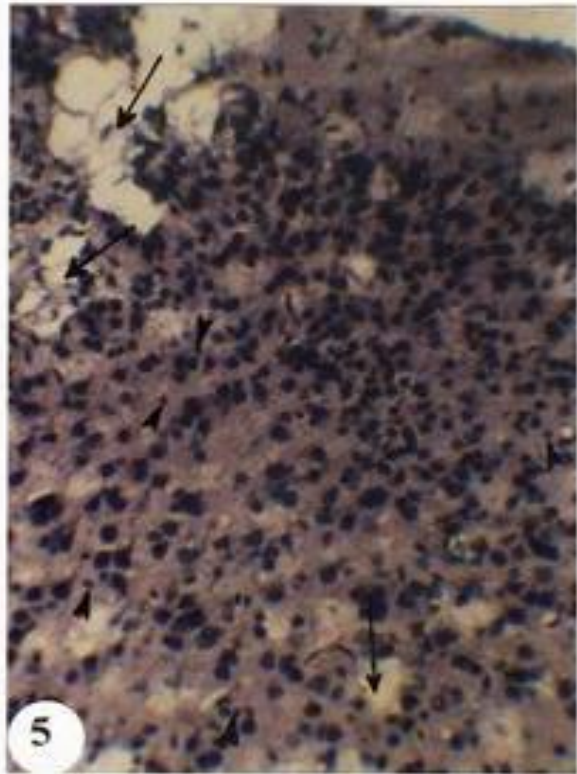
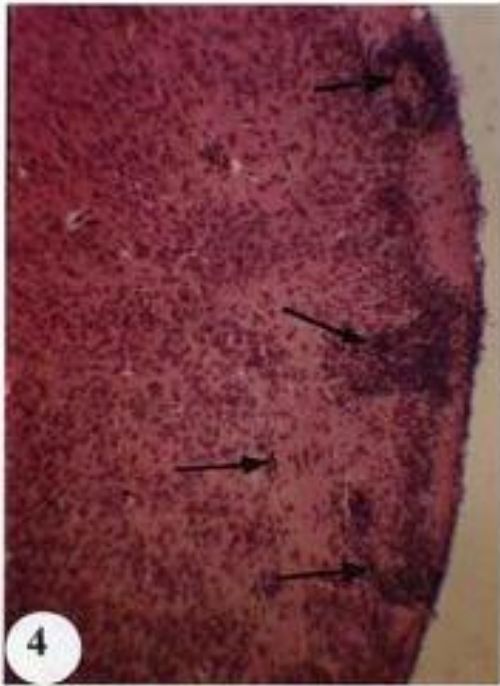
Fig. 35 : Electron micrograph showing complete loss of microvilli, rupture of apical plasma membrane (arrowhead) and blebbing (arrow) and irregular pattern of rough endoplasmic reticulum. (X 6500)

Fig. 36 : Electron micrograph showing greatly damaged paneth cells; a completely lysed one (arrow) and another with vacuolated cytoplasmic rim and irregular nucleus (arrow head). (X 4000)

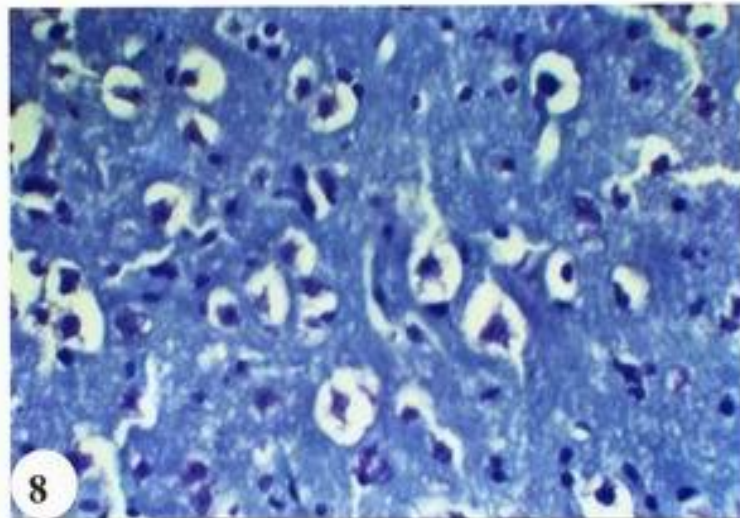
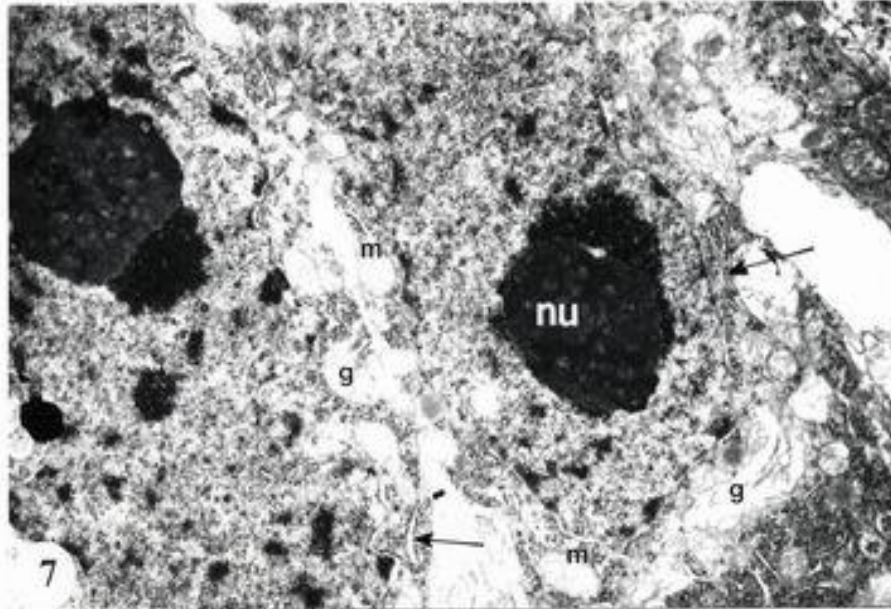
Fig. 37 : Electrophorograms showing the protein banding pattern in the brain ,pancreas and ileum in (a) heat-stressed nondiabetics (b) control (c) heat-stressed diabetics . New extrabands (arrow heads) appear clearly in case of heat stress in nondiabetics .

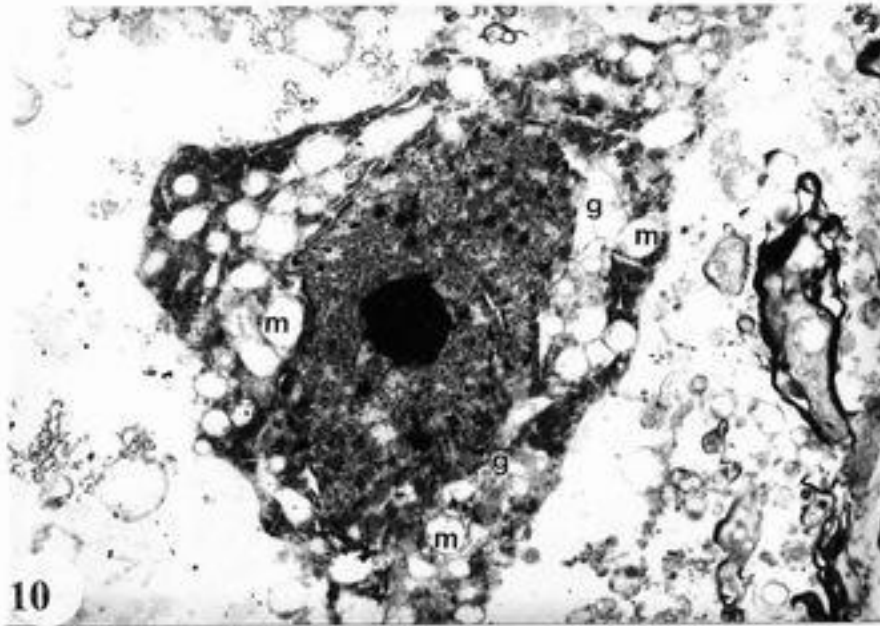
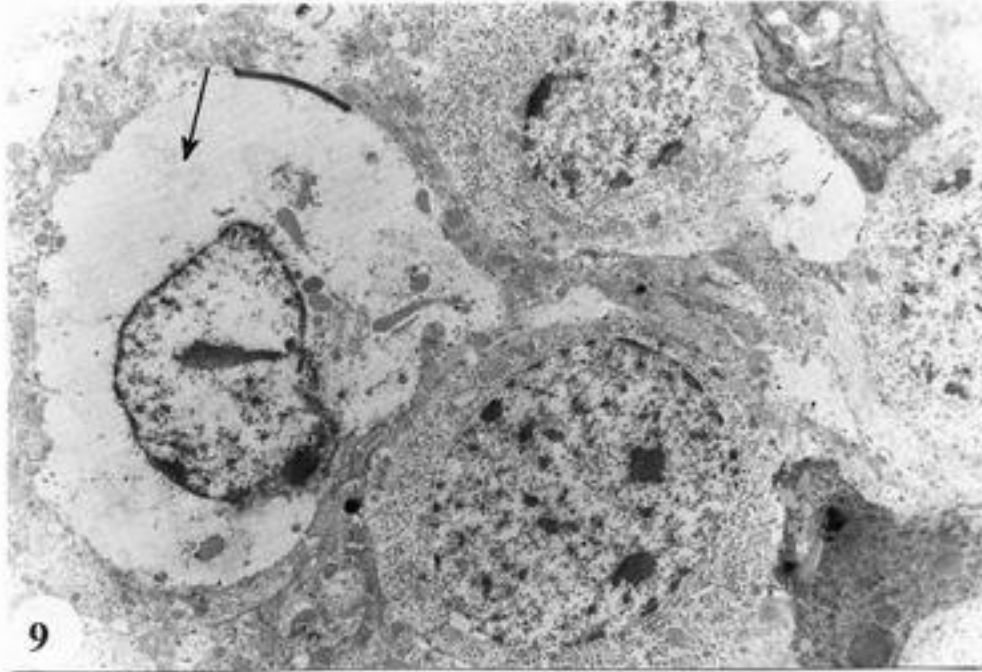
Histological and Ultrastructural Changes of the Brain.....



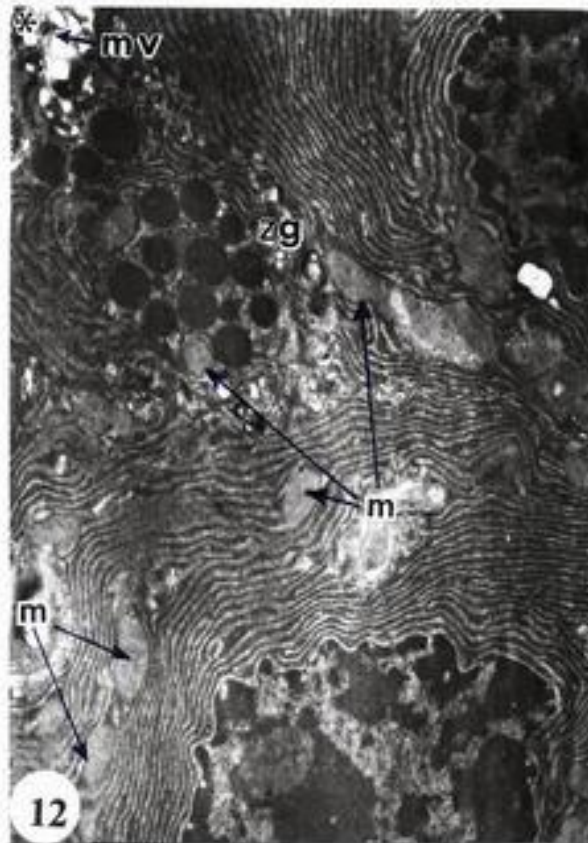
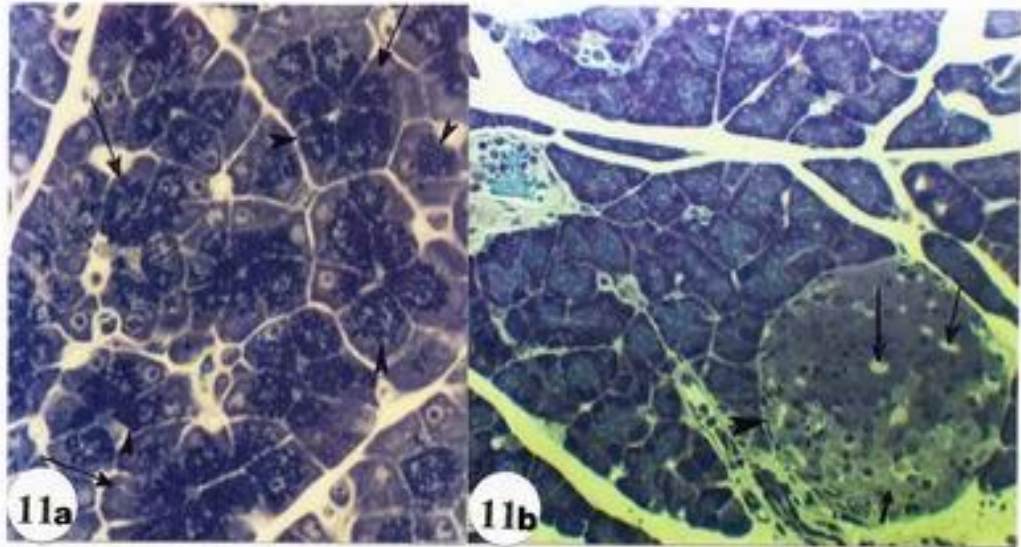


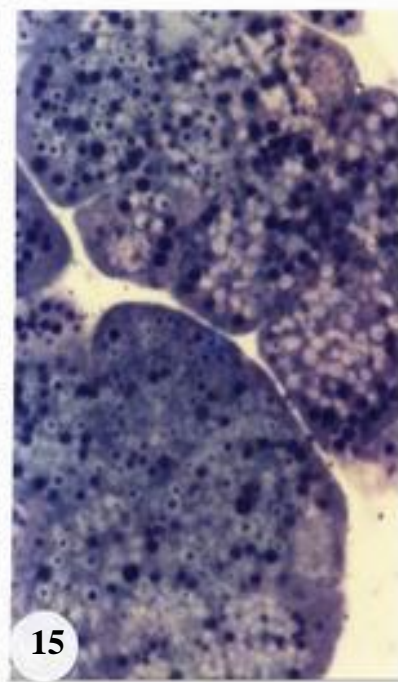
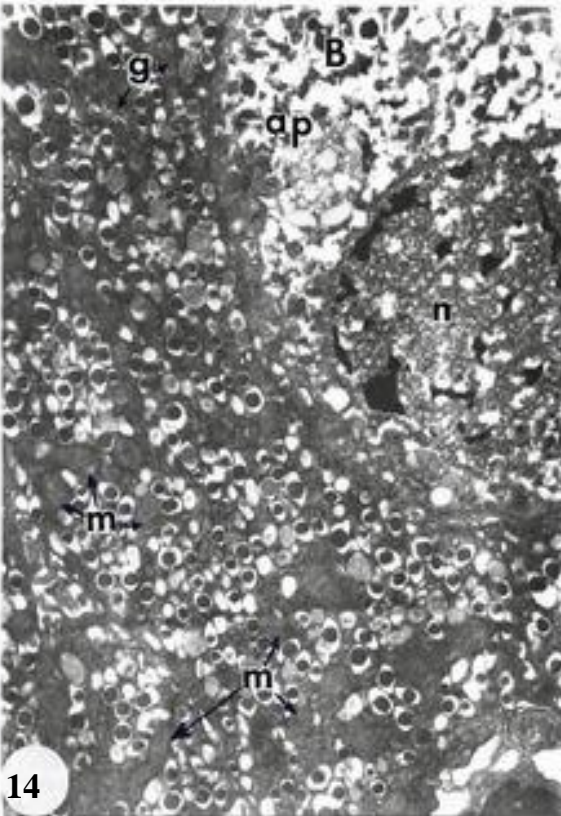
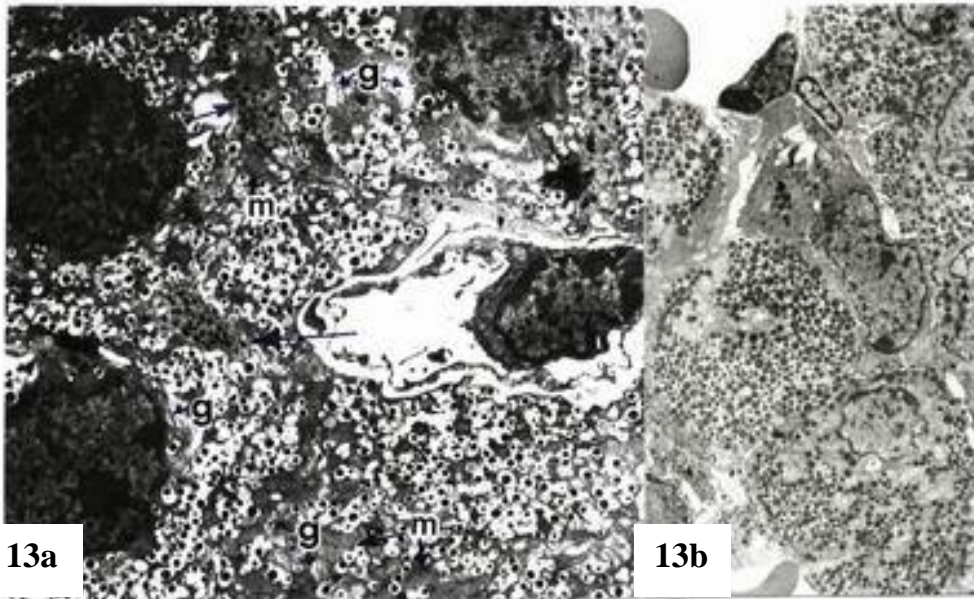
Histological and Ultrastructural Changes of the Brain.....

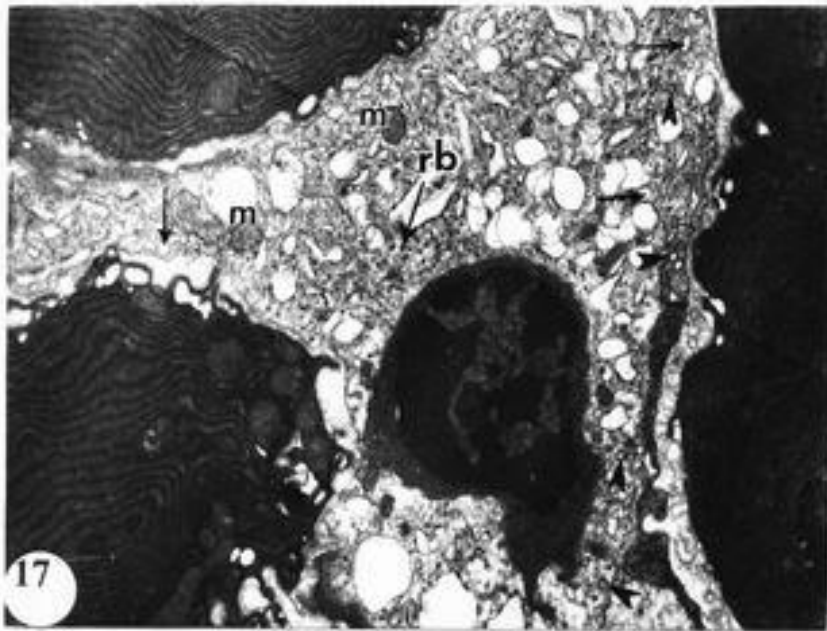
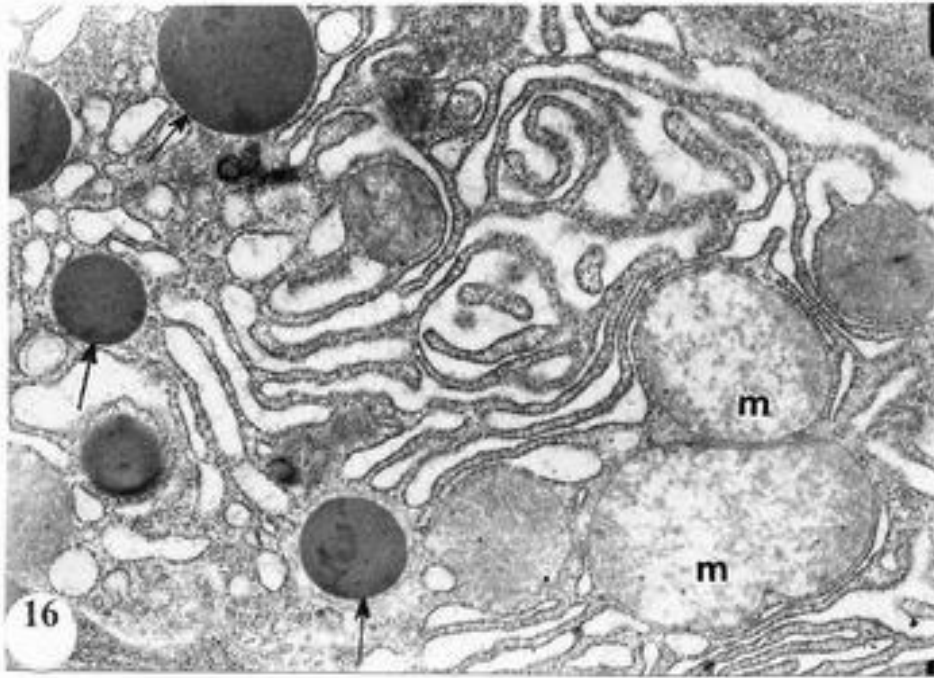


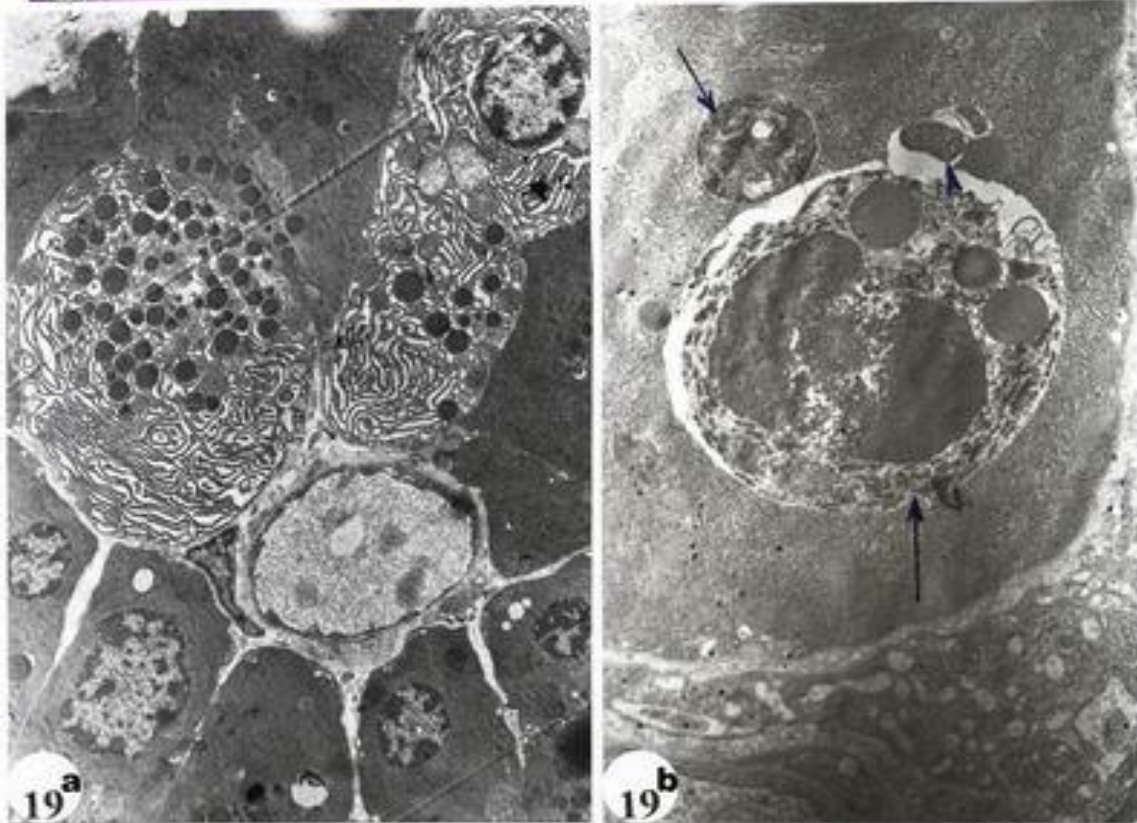
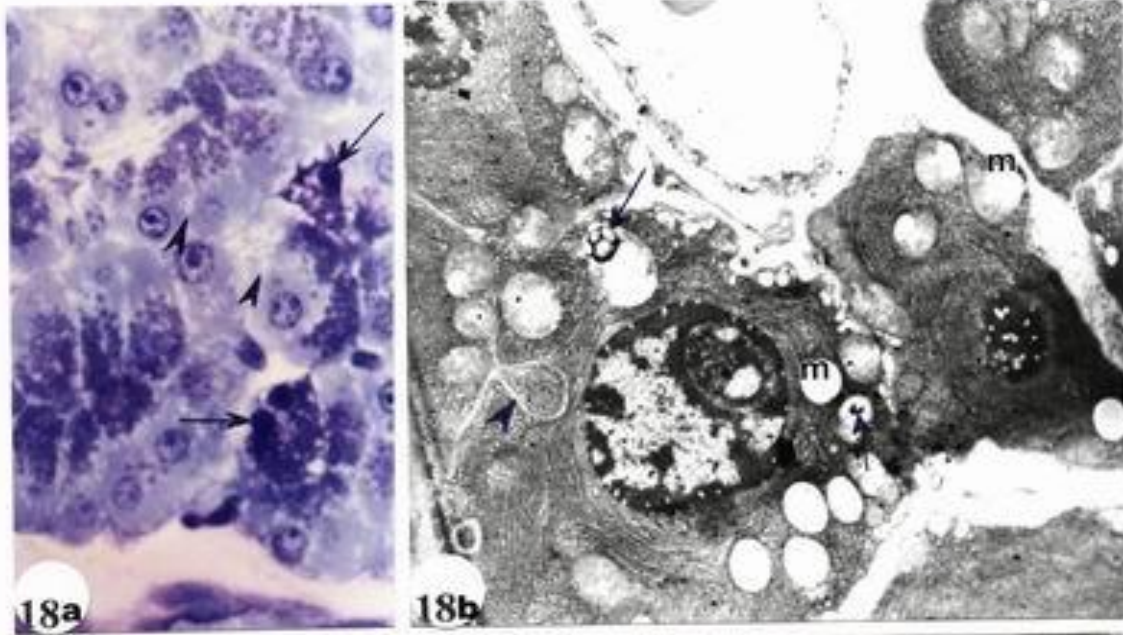


Histological and Ultrastructural Changes of the Brain.....

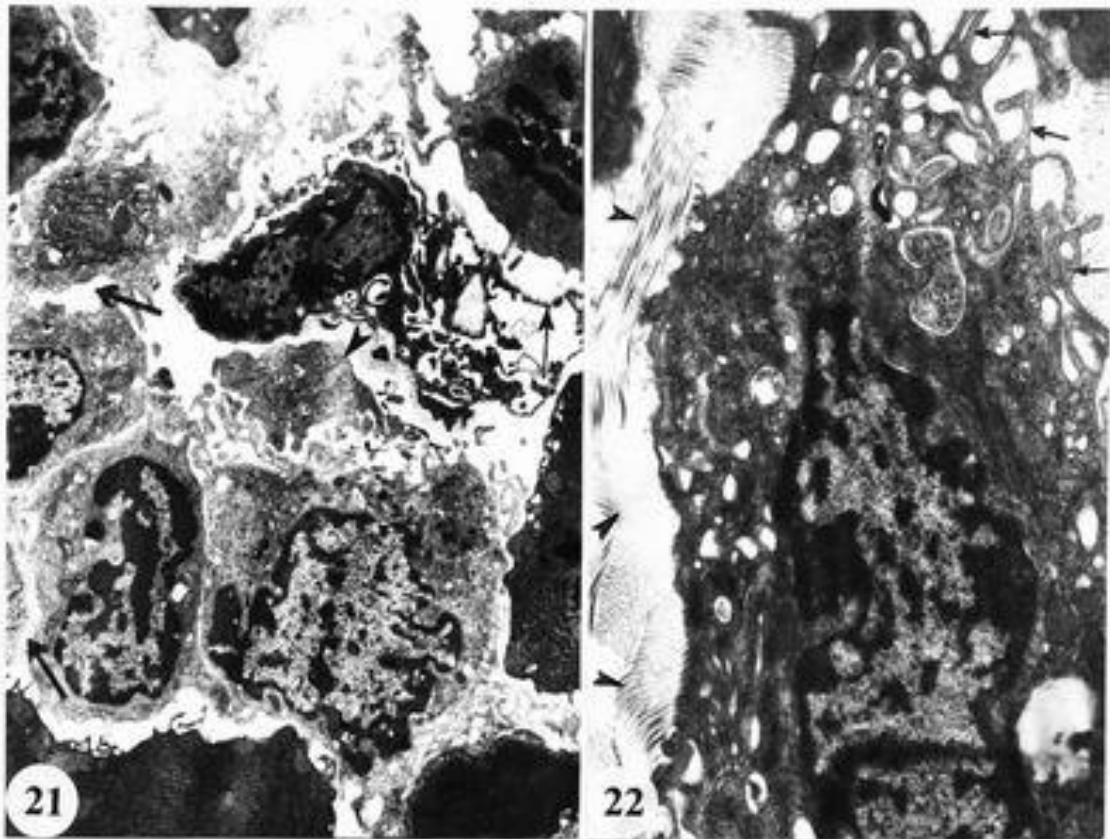
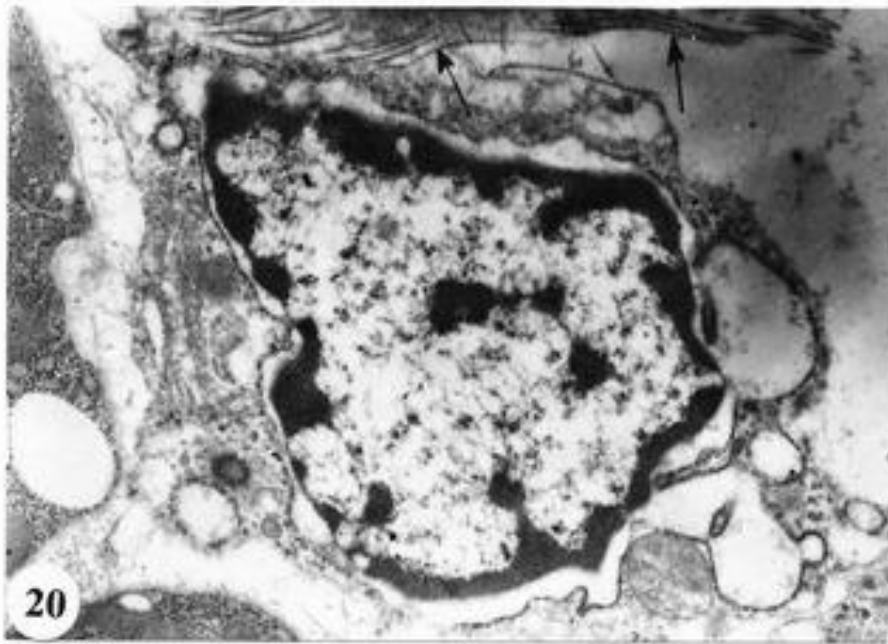


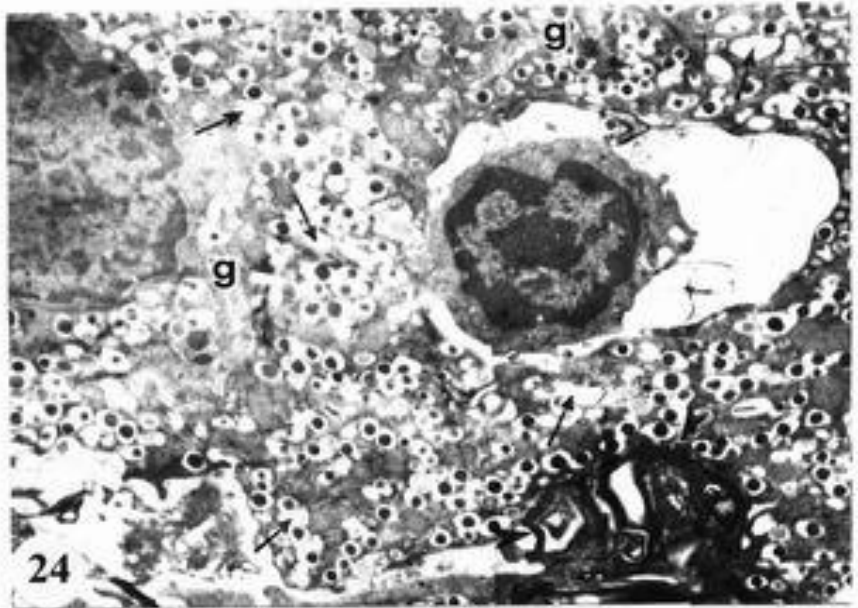
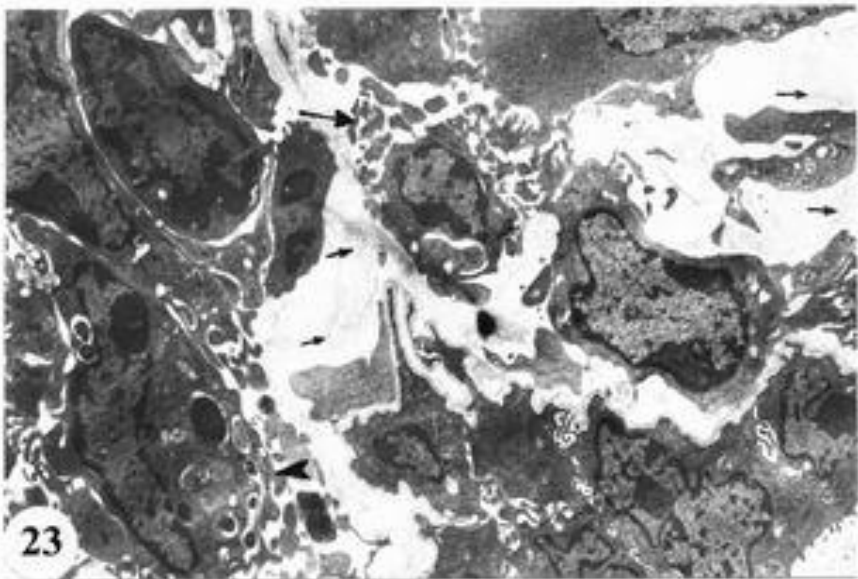




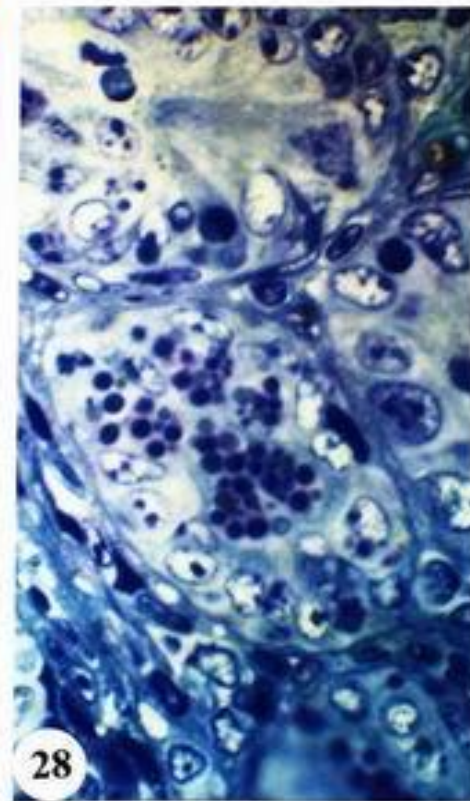
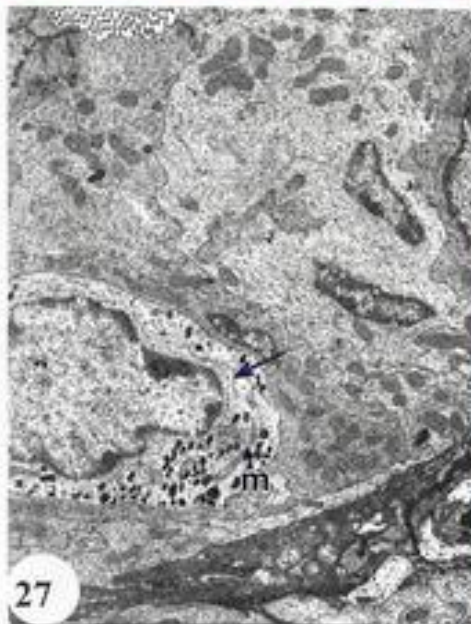
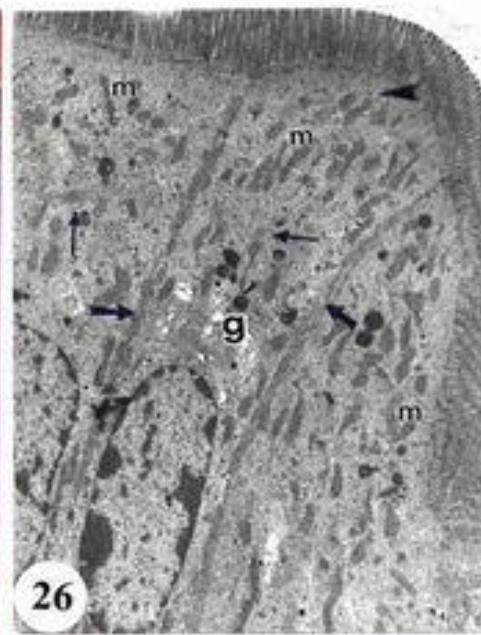


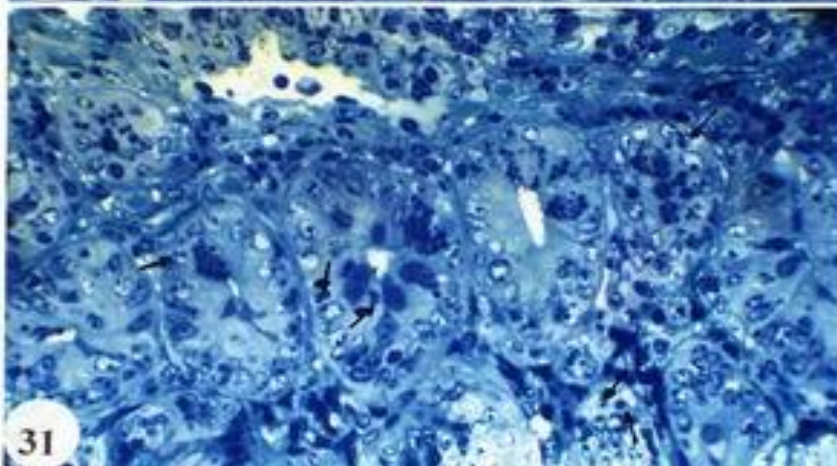
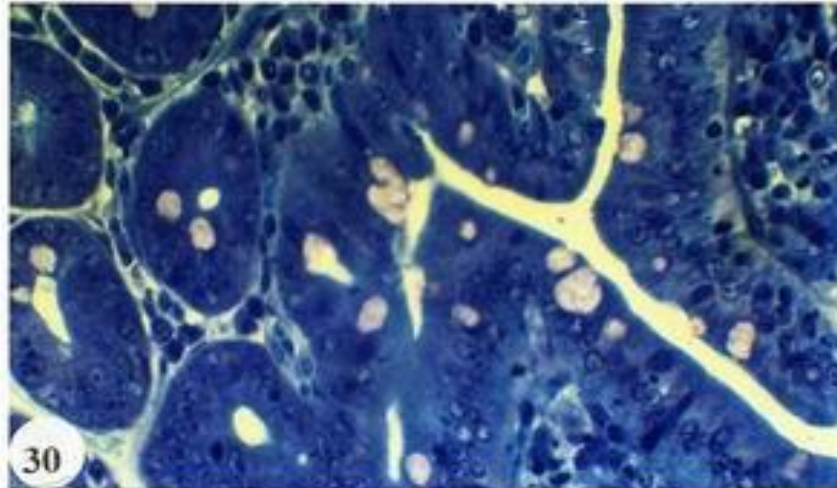
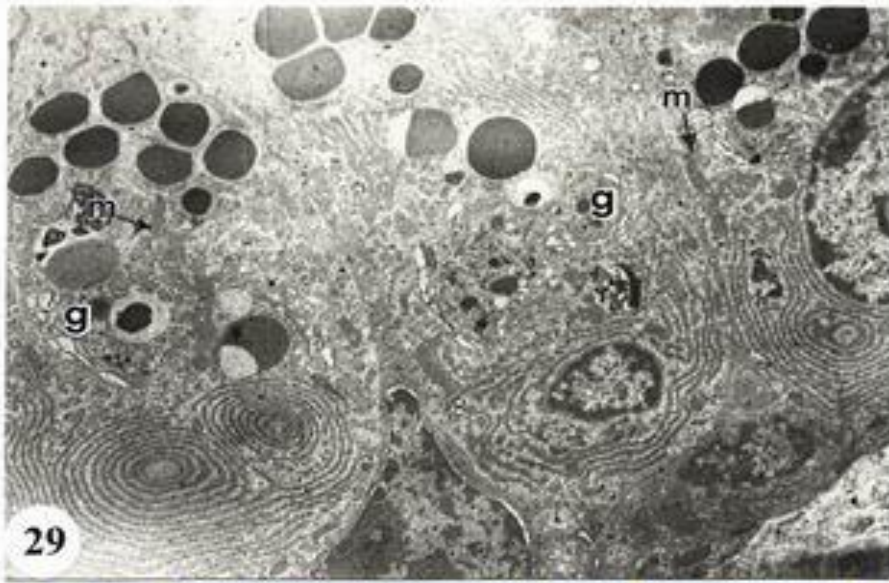
Histological and Ultrastructural Changes of the Brain.....



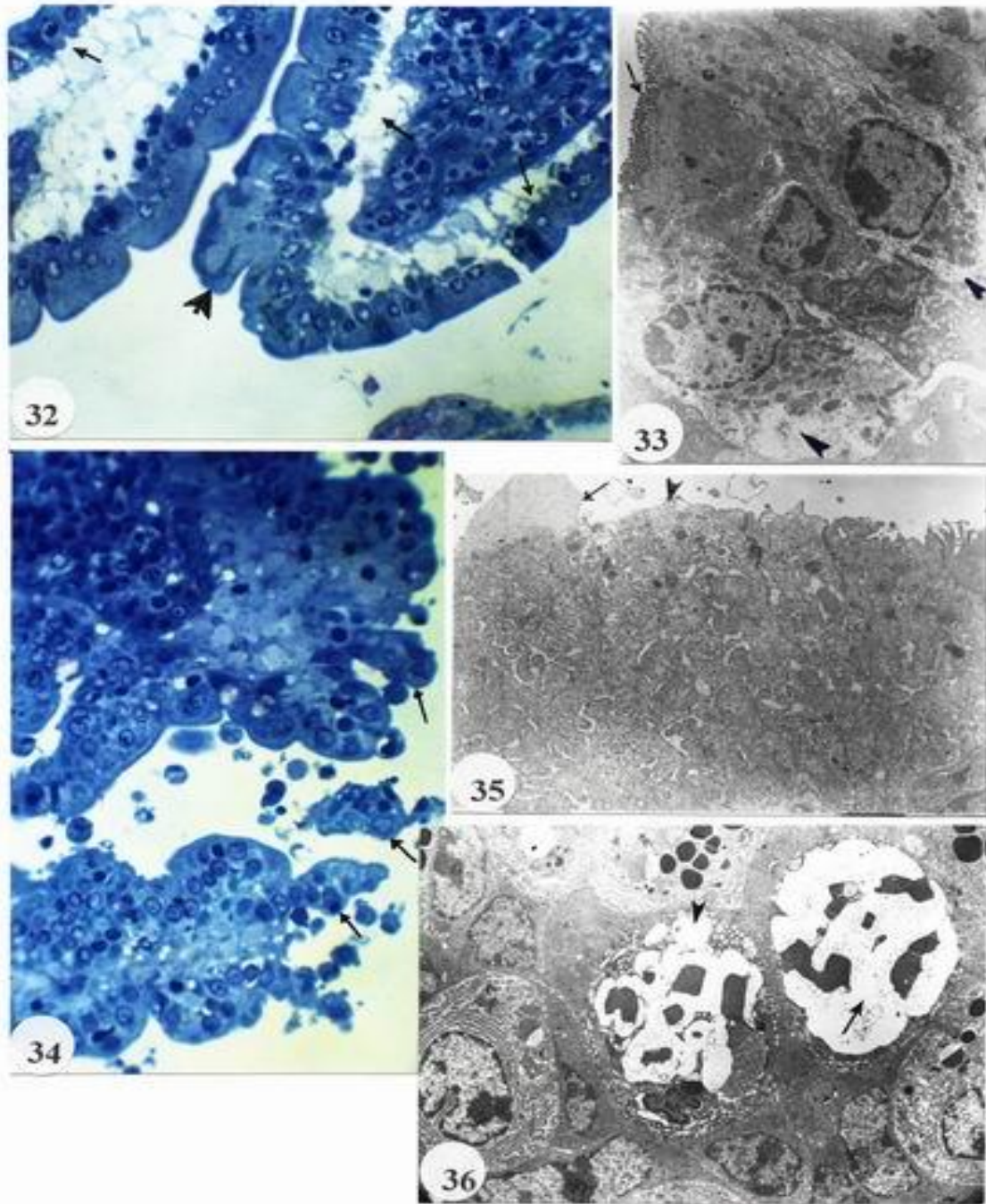


Histological and Ultrastructural Changes of the Brain.....





Histological and Ultrastructural Changes of the Brain.....



Discussion

The results presented in this paper indicate that mice with alloxan-induced diabetes didn't show any pathological changes neither in brain nor in ileum, but the only noticeable changes were noted in pancreatic islets. The islets of Langerhans were diminished in size and number, besides the B cells were specifically greatly damaged. Ultrastructural investigation showed extensive degranulation and frequent apoptosis of B cells. On the other hand A-cells and acinar cells showed no ultrastructural changes. In this respect the present results are similar to those recorded by Gopinath *et al.* (1987), Abdel-Aal *et al.* (1993) and Abdel Moneim *et al.* (1997). Moreover, the former authors stated that alloxan acts as a specific islet B-cells toxin. The nonlethal thermal stress on nondiabetic mice caused cellular and subcellular changes in the three different selected organs. However, these changes were not so drastic to be considered as generalized or comprehensive specially in brain, but in fact most of the changes were focal. On the other hand, brain, pancreas and ileum showed signs of restitution, where the brain showed increase in the number of oligodendrocytes and the ileum showed increased mitotic figures, while the pancreas showed increased interstitial cells.

The changes observed in brain under heat stress in the current study are nearly similar to those reported by Sharma *et al.* (2003), as they reported that exposure of rats to 4 hrs heat stress at 38 °C resulted in brain edema and cell damage. They concluded that oxidative stress is one of the reasons for adverse hyperthermic effect. Similarly, Sharma and Hoopes (2003) reported that morphological changes in axons, nerve cells, glial cells, and vascular endothelium were seen at the cellular and molecular levels in rats subjected to heat exposure at 38 °C for 4 hrs and that effect was dependent on age and prior thermal experience. They also added that although that regimen of heat exposure was nonfatal, it might has long-term behavioral,

physiological and neuropathological consequences.

Concerning the mechanism accounting for hyperthermia-induced injury, Friedl *et al.* (1989) stated that acute cell destruction resulting in hemoglo-binemia and hemoglobinuria immediately following thermal injury has been shown to be the result of formation of reactive oxygen products generated from activated blood neutrophils. In accordance, Till *et al.* (1989) suggested that in case of thermal injury, oxygen-derived free radicals are related to the development of acute intravascular hemolysis. Also they added that, OH⁻ might be the oxygen product involved in the generation of microvascular leakage and edema and moreover, lipid peroxidation products in thermally injured tissue. Moreover, they reported that the ability of the antioxidant enzymes catalase and superoxide dismutase to attenuate burn edema formation in thermally injured rats suggests an involvement of oxygen radicals in pathophysiological events related to thermal injury. In the study of Hall *et al.* (1999) it was found that hyperthermia produced cellular hypoxia and metabolic stress in conscious animals exposed to environmental heat stress, and they suggested that cellular metabolic stress may contribute to radical generation. Also, lowering of local cerebral glucose utilization and cerebral blood flow were considered to be the promoters for cell injury after heatstroke (Chang *et al.*, 2003). Recently (Pavlik *et al.*, 2004) considered that cerebral ischaemia and free radical formation might be involved in the initiation of cell injury during heat stress.

The occurrence of edema in nervous tissue in the present study can be ascribed to the increased blood flow and increased permeability of the vascular endothelium. The same conclusion was reported before by Till *et al.* (1989) in their study of the thermal injury of skin. Sharma *et al.* (1997) suggested that the three potent neurochemicals; serotonin, prostaglandins and

Histological and Ultrastructural Changes of the Brain.....

opioids act as mediators of the edema formation and cell pathology in hyperthermic brain injury. The swelling of mitochondria associated with loss of cristae and hypertrophy of Golgi sacs observed here might be ascribed to the occurrence of edema and the disturbance in metabolic reactions.

The current ultrastructural study showed that thermal effects on pancreas and ileum of the nondiabetic mice are to some extent similar to those found in brain. This finding seems to coincide with the statement of Karnaukh *et al.* (2004), that hyperthermia induce similar shock reaction in all organs, with systemic disorders of microcirculation. This similarity was represented by swelling and degeneration of the mitochondria, and in some cases dilation of the rough endoplasmic reticulum, which can be considered as signs of edema. The depletion of zymogen granules in heat stressed mice indicates rapid discharge of the pancreatic enzymes. Increased release of pancreatic enzymes was reported by Geokas *et al.* (1985) to be associated with edema. But it has to be mentioned that rough endoplasmic reticulum showed some resistance and was frequently seen intact in the affected cells .

In response to heat stress the pancreas showed a proliferative response through the increased appearance of interstitial cells inbetween the affected acinar cells. A similar finding was reported before by Sambasiva *et al.* (1989) in their study of copper deficiency and its role in changing the cytoarchitecture of the pancreas. They found a correlation between acinar cell loss, the proliferative response of ductular epithelium, and the appearance of interstitial cells. The ultrastructural changes recorded in the pancreas in the current study, are greatly close to structures with similar ultrastructural morphology noted in pancreas in zinc toxicosis (Kazacos and Van Vleet, 1989). According to the same opinion of the latter authors, intracisternal sequestration noted in the present study can be considered responsible for the elimination and degradation of excess membranes and organelles in acinar cell atrophy .

As reported by Haschek and Rousseaux (1991) the non proliferating villous enterocytes (absorptive cells) are more susceptible to thermal injury than the crypt cells. They reported that this injury is usually associated with histological manifestations such as swollen enterocytes, loss of microvilli and extrusion of cells from the villous tips. This might be ascribed to the more exposure of the absorptive cells and their direct contact with radicals that might be formed during thermal shock. Most of these forms of injury were to a great extent similar to those noted in the current study. However, increase of the mitotic figures was recorded in the present investigation, and that seems to be in support to the idea that mammalian intestinal epithelial cells respond to hyperthermia by inducing cytoprotection (Malago *et al.*, 2002). The latter authors mentioned that the cytoprotection involves inhibition of the proinflammatory cytokine production and induction of cellular proliferation for restitution of the damaged epithelium.

In diabetic heat-stressed mice, hyperthermia was so much destructive that various forms of damage were seen in all the three selected organs but it was much severe in pancreas and ileum than in brain. This coincide with the statement of Geokas *et al.* (1985) that the pancreas and mucosa of the gastrointestinal tract are the most rapidly autolysed body tissues. This is because cells undergoing mitosis are extremely heat sensitive due to the aggregation of globular proteins in the spindle apparatus or the disarrangement of spindles, resulting in inability to complete the mitotic division (Haschek and Rousseaux, 1991). This is why the neoplastic tissues are more sensitive to thermal effect than the normal tissues.

Comparable with the nondiabetic heat-stressed mice, the stressed diabetics were so sensitive to the thermal damaging effect. These results suggest the increased potential damaging effect of thermal stress in diabetics. This conclusion is in agreement with Change *et al.* (2003) and Niu *et al.* (2003) who reported that both Magnolol (an active component with antidiabetic effect) and insulin, respectively

were helpful in the attenuation and prevention of heatstroke damaging effect in streptozotocin – diabetic rats. Moreover, it was reported that heat shock significantly increased mortality rate in streptozotocin-diabetic rats (Swiecki *et al.*, 2003). Thus it can be concluded that diabetes lowers heat shock tolerance.

The reasonable question that should be asked is that why diabetic animals were more sensitive to the thermal stress than the nondiabetics ? The protein studies achieved by the method of polyacrylamide gel electrophoresis in the present study showed a very important phenomenon which is the appearance of new extraprotein bands in the electrophorograms of heat-stressed nondiabetic mice and the attenuation of the expression of these bands in diabetic heat-stressed animals. It is of interest that these new bands correlates well with a family of proteins called heat shock proteins (HSPs), also called stress proteins. They are a group of proteins that are present in all cells in all forms of life and are induced when a cell is subjected to various types of environmental stress like heat, cold, oxygen deprivation (Nishimura *et al.*, 1988), metallic toxicity (Zhang *et al.*, 2002) or even in some cases of cancer such as human gliomas (Hermisson *et al.*, 2004). The most commonly noted HSPs are 68 -, 70 -, 89 -, and 110 kilodalton proteins (Subjeck and Shyy, 1986).

The possible protective role of heat shock proteins was suggested as it was reported that heat tolerance and the synthesis of these proteins are coincidental (Subjeck and Shyy, 1986). Also, it was reported that they can modulate stress-induced apoptosis (Buzzard *et al.*, 1998), mediates the thermal stress-induced protection against pancreatitis (Bhagat *et al.*, 2002) and provide protection against intestinal mucosal injury during ischemia – reperfusion (Fleming *et al.*, 2002). Based on these previous reports and the present data, it can be suggested that there is a relation between the expression of heat shock proteins and the heat stress tolerance. Moreover, the attenuated expression of HSPs in brain, pancreas and ileum in the diabetic animals might be correlated with

the severity of cell injury in these organs. This assumption is in agreement with the results of Atalay *et al.* (2004) who suggested that diabetes impairs HSP protection, possibly via transcriptionally mediated mechanisms, as it decreased HSP72 expression in heart, liver and muscles in diabetic rats. It is also in agreement with the recent reports of Koranyi *et al.* (2004) who reported a correlation between heat stress proteins and diabetes and the conclusion that induction of diabetes decreases HSP72 expression in rats.

It is worthy to mention that it was reported that HSP70 was detected in rabbit hypothalamus, hippocampus and cerebral cortex (Tan *et al.*, 1997) and even in oligodendrocytes, astrocytes and vascular cells in rats (Pavlik *et al.*, 2004). This might explain the reported increase in the number of oligodendrocytes in the current study which might play an important role in attenuating the thermal stress effect. Further molecular genetic studies are needed for more understanding of the mechanism responsible for the biosynthesis of these stress proteins and their protective role.

References

1. **Abdel- Aal, W.E.; Abdel-Nabi, I.M.; Hanna, R.A. and Mahdy, K.A. (1993)** : Biochemical and histopathological changes in normal and alloxan-diabetic rats after Lupine seeds administration. *J. Egypt. Ger. Soc. Zool.*, 10 (A) : 251-267.
2. **Abdel Moneim, A.; El-Feiki, M. and Salah, E. (1997)** : Effect of *Nigella sativa*, fish oil and glioclazide on alloxan-diabetic rats : Biochemical and histopathological studies. *J. Egypt. Ger. Soc. Zool.*, 23 A : 237-265.
3. **Atalay, M.; Oksala, N.K., Laaksonen, D.E. et al. (2004)** : Exercise training modulates heat shock protein response in diabetic rats. *J. Appl. Physiol.*, 97 (2) : 605 – 611.
4. **Bhagat, L.; Singh, V.P.; Song, A.M. et al., (2002)** : Thermal stress-induced HSP70 mediates protection against intrapancreatic trypsinogen activation and acute

Histological and Ultrastructural Changes of the Brain.....

- pancreas-titis in rats. *Gastroenterology*, 122 (1) : 156-165.
5. **Bennett, H.S.; Wyrick, A.D.; Lee, S.W. and McNeil, J.H. (1976)** : Science and art in preparing tissues embedded in plastic for light microscopy, with special reference to glycol methacrylate, glass knives and simple stains. *Stain Technol.* 51 (2) : 71 – 97 .
 6. **Buzzard, K.A.; Giaccia, A.J.; Killender, M. and Anderson, R.L. (1998)** : Heat shock protein 72 modulates pathways of stress-induced apoptosis. *J. Biol. Chem.*, 273 (27) : 17147-17153.
 7. **Chang, L.; Huang, Y. and Lin, M. (2003)** : Local cerebral glucose utilization decreases after heatstroke onset in rats. *Neurosci. Lett.*, 308 (3) : 206-208.
 8. **Fleming, S.D.; Starnes, B.W.; Kiang, J.G. et al. (2002)** : Heat stress protection against mesenteric I/R-induced alterations in intestinal mucosa in rats. *J. Appl. Physiol.*, 92 (6) : 2600-2607.
 9. **Friedl, H.P.; Till, G.O.; Trentz, O. and Ward, P.A. (1989)** : Roles of histamine, complement and xanthine oxidase in thermal injury of skin. *Am. J. Pathol.* 135 (1) : 203-217.
 10. **Gabriel, J.E.; da Mota, A.F.; Boleli, I.C.; Macari, M. and Coutinbo, L.I. (2002)** : Effect of moderate and severe heat stress on avian embryonic HSP 70 gene expression. *Growth Dev. Aging*, 66 (1) : 27 – 33.
 11. **Geokas, M.C.; Baltaxe, H.A.; Banks, P.A. et al (1985)** : Acute pancreatitis . *Annals Intern. Medicine*, 103 : 86 – 100.
 12. **Gopinath, C.; Prentice, D.E. and Lewis, D.I. (1987)** : Current histopathology. Vol 13, MTP Press limited, Lancaster.
 13. **Hall, D.M.; Baumgardner, K.R. and Oberley, T.D. (1999)** : Splanchnic tissues undergo hypoxic stress during whole body hyperthermia. *J.Biol. Chem.*, 276 : 1195-1203.
 14. **Haschek, W. M. and Rousseaux, C.G. (1991)** : Handbook of Toxicologic Pathology. Academic Press Inc., London pp : 1039-1045 .
 15. **Heikkila, R.E. and Cabbat, F.S. (1980)** : The prevention of alloxan-induced diabetes by amygdalin . *Life Science*, 28 ;659-662 .
 16. **Hermisson, S.H.; Frank, D.M. and Meyermann, W.M. (2004)** : Heat shock protein expression in human gliomas. *J.Biol. Chem.*, 296 (11) : 1190-1202.
 17. **Karnaikh, N.G.; Filipchenko, L.L.; Koval, T.A.; Bilyk, L.I. and Levina, E.V. (2004)** : Morphologic changes due to hyperthermia (experimental study). *Med. Tr. Prom. Eksp.*, 5 : 17-20.
 18. **Kazacos, E.A. and Van Vleet, J.F. (1989)** : Sequential ultrastructural changes of pancreas in zinc toxicosis in ducklings. *Am. J. Pathol.* 134 (3) : 581-595.
 19. **Kelty, J.D.; Noseworthy, P.A.; Feder, M. E. and Ramirez, I.M. (2002)**: Thermal preconditioning and heat-shock protein72 preserve synaptic transmission during thermal stress . *J.Neurosci.*,22(1):193-198 .
 20. **Koranyi, L.; Hegedus, E.; Peterfal, E. and Kurucz, I. (2004)** : The role of HSP60 and HSP70 Kda heat shock protein families in different types of diabetes mellitus. *Orv. Hetil.*, 145 (9) : 467-472.
 21. **Laemmli, U.K. (1970)**: Cleavage of structural proteins during the assembly of the head of bacteriophage T4 . *Nature*, 227:680-685.
 22. **Malago, J.J.; Koninkx, J.F. and Van Dijk, J.E. (2002)** : The heat shock response and cytoprotection of the intestinal epithelium. *Cell Stress Chaperones*, 7 (2) : 191-199.
 23. **Neuhoff, V.; Arold, N.; Taube, D. and Ehrhardt, W. (1988)** : Improved staining of proteins in polyacrylamide gels including isoelectric focusing gels with

- clear background at nanogram sensitivity using coomassie brilliant blue G-250 and R-250. Electrophoresis, 9: 255-262.
24. **Nishimura, R.N.; Dwyer, B.E.; Welch, W. et al. (1988):** The induction of the major heat-stress protein in purified rat glial cells. *J. Neurosci Res.* 20 : 12-18.
 25. **Niu, C.S.; Lin, M.T.; Liu I.M. and Cheng, J.T. (2003) :** Role of striatal glutamate in heatstroke-induced damage in streptozotocin – induced diabetic rats. *Neurosci lett.*, 348 (2) : 77-80.
 26. **Pavlik, A.; Aneja, I.S.; Lexa, J. and Al Zoabi, B.A. (2004) :** Cerebral ischaemia following heat stress in the rat. *Brain Res.*, 982 (2) : 179-189.
 27. **Sambasiva, M.; Dwivedi, R.S.; Yeldani, A.V. et al. (1989) :** Role of periductal and ductular epithelial cells of the adult rat pancreas in pancreatic hepatocyte lineage. *Am.J. Pathol.* 134 (5) : 1069 – 1086.
 28. **Scharanberg, K. (1954):** Silver impregnation of astrocytes . In: *Manual of histological demonstration techniques* , p 189; H.C.Cook, Filmt, Ed Butterworths & Co. Ltd . London .
 29. **Sharma, H.S. and Hoopes, P.J. (2003) :** Hyperthermia induced pathophysiology of the central nervous system. *Int. J. Hyperthermia*, 19 (3): 325-354.
 30. **Sharma, H.S.; Drieu, K. and Westman, J. (2003) :** Antioxidant compounds attenuate brain edema formation and hemoxy-ygenase expression following hyperthermic brain injury in rat. *Acta Neurochem. Suppl.*, 86 : 313-319.
 31. **Sharma, H.S.; Westman, J.; Cervos, N.J. and Nyberg, F. (1997) :** Role of neurochemicals in brain edema and cell changes following hyperthermic brain injury in rat. *Acta Neurochem. Suppl.*, 70 : 269-274.
 32. **Subjeck, J.R. and Shyy, T.T. (1986) :** Stress protein systems of mammalian cells. *Am. J. Physiol.* 250 : 1-17.
 33. **Swiecki, C.; Strojadinovic, A.; Anderson, J.; Zhao, A.; Dawson, H. and Shea-Donhue, T. (2003):** Effect of hyperglycemia and nitric oxide synthase inhibition on heat tolerance and induction of heat shock protein 72 KDa in vivo. *Am.Surg.*, 69 (7) : 587 – 592.
 34. **Tan, M.; Hua, X and Qiu, R. (1997) :** Distribution of 70 Kda heat shock protein in rabbit brains after heat stress and heat stroke. *Zhonghua Bing Li Xue Za Zhi.*, 26 (1) : 38-40.
 35. **Till, G.O.; Guilds, L.S.; Mahrougi, M. et al. (1989) :** Role of xanthine oxidase in thermal injury of skin. *Am.J. Pathol.* 135 (1) : 195-202.
 36. **Weil, A. and Davenport, H.E. (1933) :** Oligodendrocytes and microglia in silver impregnation techniques . In: *Manual of histological demonstration techniques* , p 170,171 ; H.C.Cook, Filmt, Ed. Butterworths & Co. Ltd . London .
 37. **Zhang, B.Y., Chem, S.; Ye. F.L. et al. (2002) :** Effect of manganese on heat stress protein synthesis of new-born rats. *World J.Gastroenteral.*, 8 (1) : 114-118.

**التغيرات النسيجية و التركيبية الدقيقة فى المخ و البنكرياس و اللفائفى فى الفئران
المصابة بداء السكرى والغير مصابة تحت تأثير الاجهاد الحرارى مع اشارة خاصة
لبروتينات الاجهاد الحرارى**

حمدى حامد سويلم

قسم علم الحيوان - كلية العلوم- جامعة عين شمس

صممت هذه الدراسة لتقييم تأثير الاجهاد الحرارى على المخ و البنكرياس و اللفائفى فى الفئران الطبيعية و تلك المصابة بداء السكرى (عن طريق الحقن بمادة الألوكسان) و ذلك من خلال دراسة التغيرات التركيبية علمستوى الميكروسكوب الضوئى و الألكترونى وكذلك دراسة التغيرات الجزيئية من خلال فحص التغيرات فى أشرطة البروتينات التى ظهرت فى صور الفصل الكهربائى لهلام عديد الأكريلاميد فى مجموعات الفئران المختلفة . و لقد قسمت الحيوانات الى أربع مجموعات : المجموعة الضابطة , المجموعة المصابة بداء السكرى عن طريق الحقن بالألوكسان , المجموعة المعرضة للاجهاد الحرارى و غير مصابة بداء السكرى , و المجموعة المصابة بداء السكرى و تم تعريضها للاجهاد الحرارى .

ولم تلاحظ أية تغييرات جوهريّة فى الحيوانات المصابة بداء السكرى و التى لم يتم تعريضها للاجهاد الحرارى سوى بعض التغيرات التركيبية الدقيقة فى خلايا (ب) بجزر لانجرهانز فى البنكرياس . وقد أظهرت الحيوانات الغير مصابة بالسكرى و التى عرضت للاجهاد الحرارى تغيرات خلوية و تحت خلوية فى الأعضاء محل الدراسة و التى كانت فى معظمها بؤرية . وقد ظهرت دلالات على التعويض فى الثلاث أعضاء المختارة بعد التعرض للاجهاد الحرارى . وعلى الجانب الآخر فقد وجد أن الأجهاد الحرارى كان مدمرا الى حد كبير فى الحيوانات المصابة بداء السكرى وقد ظهر ذلك جليا فى البنكرياس . وقد وجد أن الاختلاف فى درجات الأضرار الخلوية

الناجمة عن الاجهاد الحرارى بين الحيوانات المصابة بالسكرى و الغير مصابة مرتبط بالنتائج المتحصل عليها من دراسة البروتين والتى اوضحت أن الحيوانات الغير مصابة بالسكرى أظهرت تعبيراً أكثر لبروتينات الاجهاد الحرارى عن تلك المصابة بداء السكرى . و يعتقد بأن هذه البروتينات قد تلعب دوراً هاماً فى الحماية من أضرار الاجهاد الحرارى . و متمشياً مع هذا الاعتقاد فقد وجد أن المخ والذى أظهر مقاومة أكبر ضد الاجهاد الحرارى هو الذى أظهر تعبيراً أكثر لهذه البروتينات عن باقى الأعضاء . و زيادة على ذلك فان الانخفاض فى تكوين هذه البروتينات فى حالة الاصابة بالسكرى يزيد من دعم الاقتراح بأن داء السكرى يوهن الاستجابة للاجهاد و يضعف من تكوين هذه البروتينات المقاومة للاجهاد الحرارى .

و الخلاصة أن هذا الموضوع ذو أهمية علمية و يحتاج الى دراسات اضافية لمعرفة و توصيف التركيب الجزيئى لهذه البروتينات و الجينات المسؤولة عن التعبير عن هذه البروتينات فى هذه الأنسجة و باقى أنسجة الجسم المختلفة .